IL NUOVO CIMENTO Vol. 29 C, N. 3 Maggio-Giugno 2006
DOI 10.1393/ncc/i2006-10004-4

Performance of the AMS-02 silicon detector

A. Oliva for the AMS tracker Collaboration(*)
INFN and Università di Perugia - Perugia, Italy

(ricevuto il 9 Gennaio 2006; approvato il 10 Aprile 2006; pubblicato online il 21 Giugno 2006)

Summary. — The Alpha Magnetic Spectrometer (AMS) is a high-energy particle physics experiment in space. Eight layers of double-sided silicon detectors, embedded in a 0.8 T magnetic field created by a superconducting cryo-magnet, are the core of the AMS-02 detector. With a 10 μm spatial resolution, the silicon tracker is able to measure the magnetic rigidity and the sign of the passing particle up to few TV, with a resolution of $\Delta R/R \sim 2.5\%$. In addition the energy loss of the particle in silicon enable the measurement of the absolute charge of nuclei until iron. In this work are presented, in terms of spatial and charge resolution, the performance of the silicon detector in a test beam performed in October 2003 at the CERN SPS.

PACS 07.87.+v – Spaceborne and space research instruments, apparatus, and components (satellites, space vehicles, etc.).
PACS 95.55.Vj – Neutrino, muon, pion and other elementary particle detectors; cosmic rays detectors.
PACS 29.30.Aj – Charged-particle spectrometers: electric and magnetic.
PACS 29.40.Gx – Tracking and position-sensitive detectors.

1. – Introduction

AMS is a high-energy particle physics space-borne experiment conceived for the search of primordial antimatter and the indirect search of dark matter. A first version of the device (AMS-01) was tested during a 10-day flight in June 1998 (STS-91) on the space shuttle *Discovery* [1]. A new and improved version of the apparatus, AMS-02, will operate on the International Space Station, at an altitude of 400 km above the sea level.

(*) INFN and Università di Perugia, Italy; D.N.P.C, Université de Genève, Switzerland; I.Physikalisches Institute, RWTH, Germany; CERN, Switzerland; Massachusetts Institute of Technology, USA; University of Turku, Finland; NLR, Netherlands; Moscow State University, Russian Federation; South-East University, Nanjing, China; Sun Yat-Sen University, Guangzhou, China; Groupe d'Astroparticules de Montpellier, France; Institute of Space Science of Bucharest, Rumania.

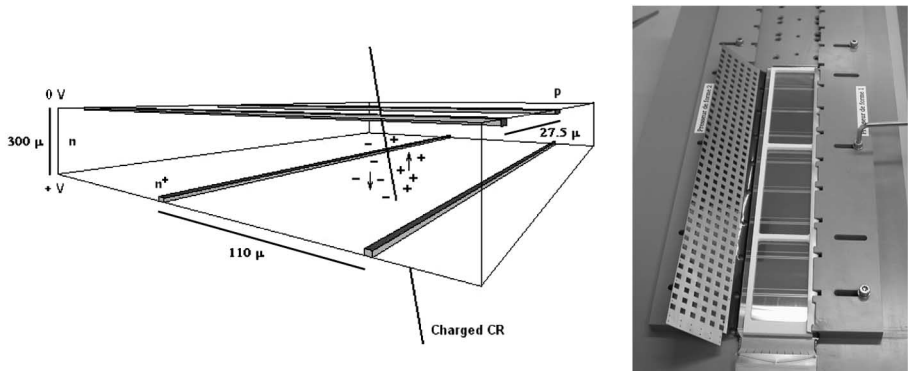

Fig. 1. – The double-sided silicon sensor, and, on the right, a ladder of the AMS tracker flight-model before the shielding phase.

It will provide a precise and accurate measurement of the spectrum of the cosmic rays in the energy range from hundred of MeV/n to few TeV/n for particle charges up to iron.

AMS-02 is designed around a central spectrometric core composed by a cryo-magnet (0.8 T magnetic field) and a eight layers silicon tracker. Two pairs of scintillator planes, placed on the top and at the bottom, of the spectrometer, constitute the time-of-flight system (TOF), which provides the charged particle trigger of the experiment and measures the velocity and the arrival direction of the impinging particles. A Ring-Imaging CHerenkov detector (RICH), an imaging Electromagnetic CALorimeter (ECAL) and a Transition Radiation Detector (TRD) complete the apparatus to allow the particle identification.

For a realistic evaluation of the tracker performances in the absolute charge (Z) and the position measurements, a beam test campaign has been carried out by the AMS-Tracker Collaboration exposing flight-model units of the detector to ion, proton, electron and photon beams. This work reports on the results obtained in the analysis of the data from ion/proton beam test carried at CERN in October 2003.

After a short introduction on the AMS-02 silicon tracker, and a brief description of the 2003 beam test, in sects. **4** and **5** are presented the calibration procedure and data selection. Finally, in sects. **6** and **7**, results in terms of charge and position measurements are presented.

2. – The silicon tracker

The tracker basic element is the double-sided silicon microstrip sensor ($\sim 72\times41$ mm^2) schematically shown in fig. 1. On the two surfaces of a high-resistivity n-doped silicon substrate, p^+ and n^+ strips are implanted along orthogonal directions. The sensor operates in a regime of inverse polarization at full depletion. When a charged particle crosses the sensor electron-hole pairs are formed. Due to the electric field holes migrate to the p-side, while electrons migrate to the n-side inducing a signal on the readout strips. Within the AMS reference system, the p^+ strips of the *junction* side run along the x direction to provide measurement of the bending coordinate (y), with an implantation (readout) pitch of 27.5 (110) μm. The n^+ strips of the *ohmic* side have a coarser implantation (readout) pitch of 52 (208) μm.

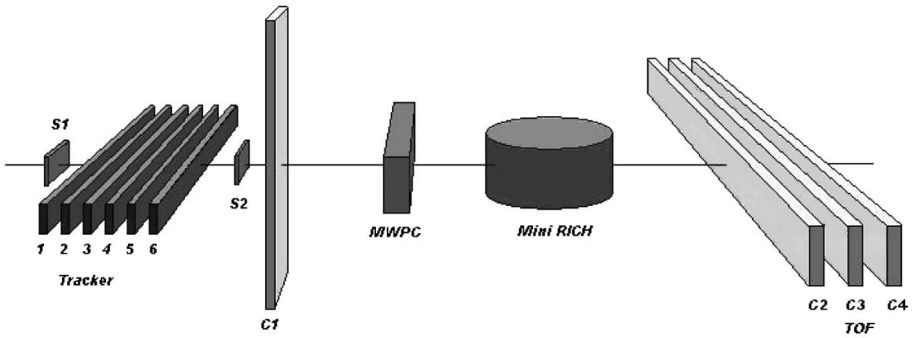

Fig. 2. – A schematic view of the October 2003 test beam set-up.

A variable number of sensor, from 7 to 15, are grouped along the x direction to form a single electrical unit, the *ladder*, readout by low noise, high dynamic range charge sensitive amplifiers VAhdr9a (an improved version of the chip used in AMS-01 [2]) placed on a hybrid board on the ladder's end. On the junction side strips of the different sensors are electrically connected along the ladder length and directly connected to the front-end electronics, resulting in 640 readout channels. On the ohmic side an L-shaped fan-out on a thin kapton foil is used to route the strip signals coming from even (odd) sensors along the ladder, keeping a total of 384 readout channels independent of the ladder length.

Ladders are disposed on eight layers of ~ 1 m diameter for an effective sensitive area of ~ 6.4 m^2 and a total of ~ 192 k readout channels. In order to keep the event size at a manageable level, an early suppression of the tracker channels with no significant signal is performed by a DSP in the online processing of the tracker data by a dedicated Tracker Reduction Data (TRD) boards.

3. – Beam test set-up

The beam test setup is sketched in fig. 2. Six flight-model ladders were placed orthogonal respect to the beam, together with four time-of-flight scintillator counters and a Cherenkov prototype (mini-RICH). The beam was generated by a 158 GeV/n Indium beam colliding on a Be target. The fragments, with an average energy of 10 GeV/n, were selected by a quadrupolar magnet fixing the A/Z ratio.

During the 10 days of the test, a total of ~ 20 millions events were acquired in 200 runs with different A/Z configuration:

- $A/Z = 1$: 6% proton events;
- $A/Z = 2$: 77% events with a dominant Helium component. Nuclei up to $Z = 26$ were present in the beam, but the Be component was suppressed;
- $A/Z = 2.25$: 16% events, enhanced ^{9}Be component;
- $A/Z = 2.35$: 1% events, enhanced ^{7}Li component and suppressed He component.

4. – Calibration and data compression

In order to perform an off-line study of data compression algorithms to be implemented in the TDR, the beam test data were readout in *raw mode*, *i.e.* signals from all

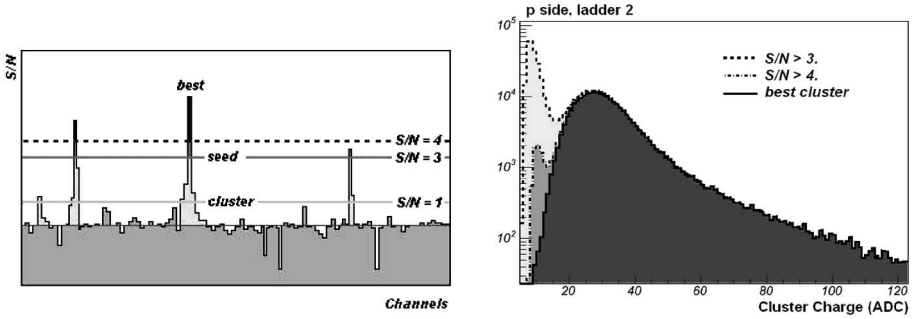

Fig. 3. – On the left an example of SN distribution after calibration procedure. The two threshold, for the seed definition and for cluster construction, are shown. Cluster-included strips are filled in dark gray. On the right is presented the total cluster charge for three different cluster selections in a proton run: (a) in light gray the pre-selection, (b) in gray the $n_{\rm seed} > 4$ selection and (c) in dark gray the *best* cluster selection.

channels were recorded, with no online filtering applied. Out of spill events were used in the offline analysis to study the channels response in absence of physical signals. This allowed the computation for each readout channel of the *pedestal* (p), defined as its average signal level. The raw ADC values of each event were corrected to remove a *common noise* contribution defined as the average ADC value on the 64 channels of each VA chip. The variance of the channel pedestal after the common noise subtraction is then defined as *noise*, *i.e.* $\sigma_{\rm ped}$. The noise receives contributions both from the the silicon sensor dark current fluctuations and the electronic noise of the readout electronics. It resulted nearly stable in the test, with a small linear increase with temperature, as expected for the silicon noise component. Channels with exhibited an anomalous behavior either because too noisy ($\sigma > 5$ ADC), dead ($\sigma < 0.1$ ADC) or with non-Gaussian noise distribution where marked as *bad* and excluded from subsequent analysis. The average noise levels in the test beam, were $\langle\sigma\rangle = 2.5(3.1)$ ADC counts on p (n) side, with a percentage of $< 1(5)\%$ of bad channels.

Due the capacitive coupling of the readout strips, a charged particle traversing the sensor induces a signal in few strips near the impact position. As a consequence, the typical signal is distributed over an ensemble of strips, the *cluster*. In the spill runs, the pedestal and common noise subtracted signal (S) value is computed for each channel. The signal over noise $SN = S/\sigma$ ratio is then used as a discriminant quantity to look for clusters. On the left of fig. 3 is presented a typical configuration of the SN for a ladder after the calibration procedure in a beam event. A signal exceeding a given threshold of $n_{\rm seed}\sigma$ is called *seed* and triggers the constitution of a new cluster, which is built associating to the seed the neighboring strips with $SN > SN_{\rm neighbor}$.

The calibration and clusterization procedures are the basis of the data compression task, which during the AMS operation will be integrated in the TDR electronics. In particular, the clusterization should be a quite conservative procedure to have full efficiency in selecting the signal event, at the price of getting also some fake clusters originating from noise fluctuations. From our proton analysis values of $n_{\rm seed} = 3$–3.5 and $SN_{\rm neighbor} = 0$–1 seem appropriate to keep a manageable data size without introducing significative inefficiencies.

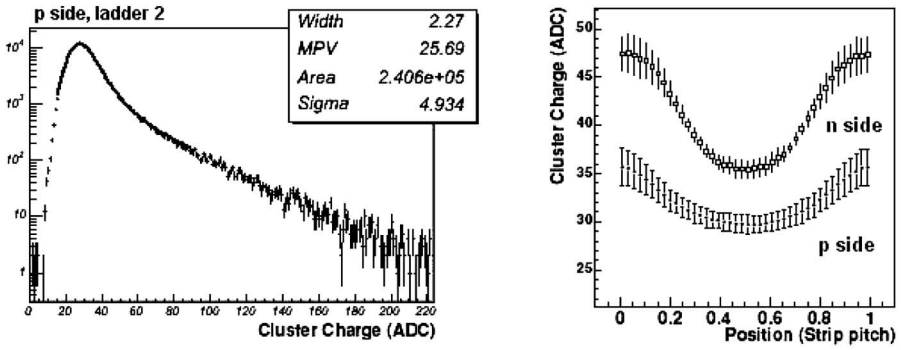

Fig. 4. – On the left the Landau-Gaussian convoluted profile of the proton energy loss. On the right the position-dependent charge collection for the p and n side, in particular $\sim 0.$ and $\sim 1.$ are positions of the 2 readout strips, while ~ 0.5 is the interstrip region.

5. – Cluster selection

The cluster amplitude, defined as the sum of cluster strips signals, is proportional to the energy loss of the traversing particle. Since the ionization energy loss is $\propto Z^2$, higher signal levels and larger strip multiplicity are expected in clusters with increasing Z of the incident particle. On average, a proton produces a cluster of 2.24 (2.05) strips for the p (n) side, with a most probable cluster charge value of ~ 30 ADC counts. This corresponds, at the single strip level, to a signal value close to the 3σ threshold, making the selection of proton clusters a quite delicate task. Conversely, a multiplicity of 4.9 (4.4) strips, with a most probable charge of ~ 100 ADC are the average characteristics for a relativistic He cluster. The seed strip in helium clusters has typically a $SN > 5$, easing the task of an efficient discrimination of such a signal from the noise background.

As an example on the right part of fig. 3 is presented the total charge obtained on the p-side in a proton run ($A/Z = 1$). The first dashed line corresponds to the pre-selected clusters ($n_{\text{seed}} = 3, SN_{\text{neighbor}} = 0$): two different peaks are clearly visible corresponding to noise generated clusters, for low charge values, and to the genuine proton signal. The dotted line corresponds to clusters with a seed greater than 4σ. With this selection the number of noise generated cluster is reduced, but some good proton clusters are lost. An effective noise rejection has been obtained by selecting, for each ladder, only the highest charge cluster: the resulting cluster charge distribution corresponds to the dark shaded area.

6. – Charge measurement

The bulk of the charge distribution is well described by a Landau distribution convoluted with a Gaussian, as can be seen in fig. 4, as expected from the characteristics of the energy loss distribution of a particle traversing a thin material. The same cluster selection has been applied on the n-side clusters, however a relevant dependence of the total collected signal has been found on the impact point of the particle relative to the position in the gap between adjacent readout strips. On the right of fig. 4 the average cluster charge collected on the two silicon sides is presented as a function of the interstrip impact position of the particle. The impact position of the particle was evaluated on the

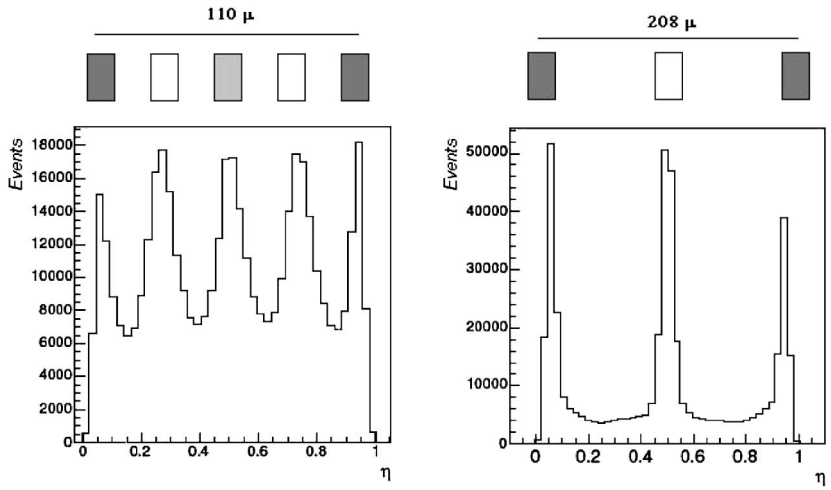

Fig. 5. – η distribution for the p-side, on the left, and for n-side, on the right. On top of the figure there is the corresponding strip implantation: (a) in gray the readout strips, (b) in light gray the metalized ones and (c) in white the non-metalized strips.

ladder under study from the reconstruction of the particle trajectory with the other five ladders of the telescope. While the p-side charge collection has a weak dependence from impact position, the charge collection for the n-side is maximum when the impact position is close to the readout strips, and is $\sim 30\%$ less in the region between two readout strips.

Due to the inter strip capacitive coupling, the reconstruction of the impact point of the particle can be defined from the cluster signal center of gravity. A good approximation of the particle coordinate is given by η defined as

$$\eta = \frac{Q_{\mathrm{R}}}{Q_{\mathrm{R}} + Q_{\mathrm{L}}},$$

where $Q_{\mathrm{L}}, Q_{\mathrm{R}}$ represent the two most energetic strips in the cluster, L or R label reflect the lower (Left) or higher (Right) channel readout number. In fig. 5 is presented the η distribution for a $Z = 2$ perpendicular incident particles for the p and the n-side. On the top of the picture is presented the implantation structure. The correlation between the strip implantation structure and the η distribution is clear. Especially on the n-side the η distribution has strong peaks and the gaps between strips are depleted, *i.e.* n-side performs a "quasi-digitalized" measurement of position with a pitch of $104\,\mu$m. For a uniform illumination of the sensors, we can therefore make a rough estimate of its spatial resolution as $d_{\mathrm{pitch}}/\sqrt{12}$, with $d_{\mathrm{pitch}} = 27,5(104)\,\mu$m on the p(n) side, leading to $\sim 8\ \mu$m for the p-side, and $\sim 30\ \mu$m for the n-side.

Should be also stressed, that the η we are presenting is relative to tracks impinging orthogonally on the detector, whereas a different charge collection in the gap is expected for inclined tracks.

Quite different η dependences of the charge collection have been found for higher Z values of the incident particle [3]. However, once this effect is measured, a set of Z-dependent corrections can be estimated on both the p and n sides and applied to

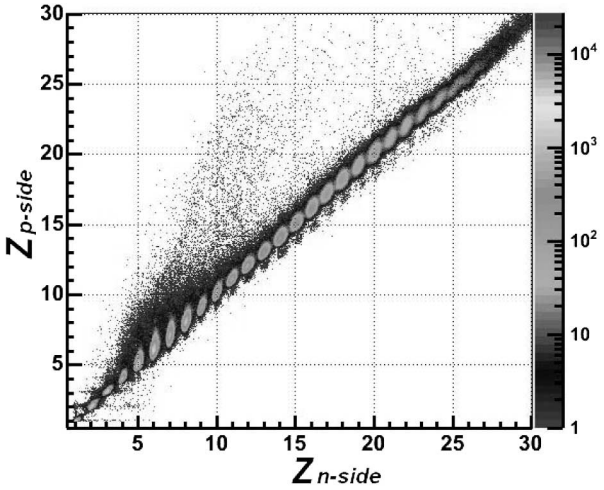

Fig. 6. – Charge measured by the two side after the correction, an effective charge separation up Fe ($Z = 26$) can be achieved.

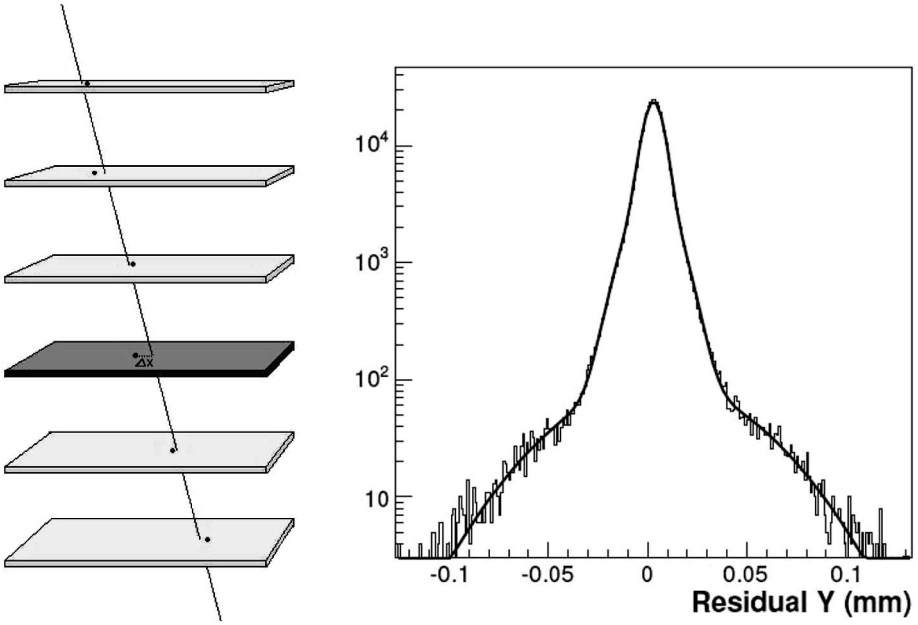

Fig. 7. – A schematic view of the residual analysis on the left. On the right the residual distribution fitted with a double Gaussian.

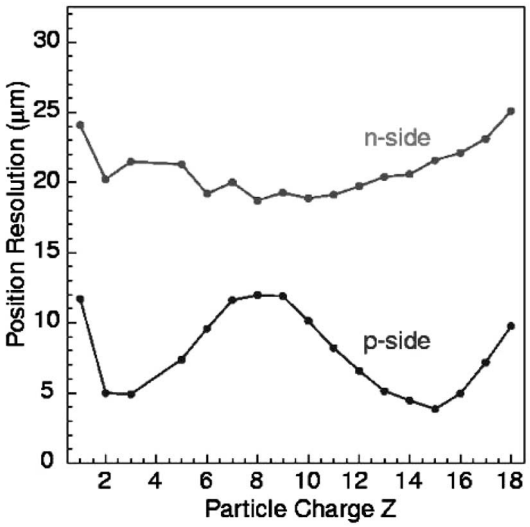

Fig. 8. – Position resolution function of particle charge. Due to the strong dependence of η distribution to Z there are many differences between the p-side resolutions, while n-side has a constant resolution of $\sim 30\,\mu$m, as expected from the quasi-digitalized form of η distribution.

recover a uniform detector response in the whole η range. After these corrections, an effective charge separation up Fe can be achieved, as shown in fig. 6.

7. – Position resolution

The main task of the AMS-02 silicon tracker is the track reconstruction of charged particles with rigidities reaching several TVs. To fulfill such a task, the required resolution in the single point measurement on the bending plane (p side) is ~ 10 μm. One of the main objectives of this test beam was to verify that such a resolution could be effectively achieved with the flight ladders and readout electronics.

In the beam test, the single point resolution was evaluated for each ladder from the distribution of the residuals between the position measurement, given by η, and the predicted impact position of the particle as evaluated from a fit to a straight line using the position measurements of the remaining five ladders (see fig. 7).

Since the residual is defined as

$$\Delta x_{\text{residual}} = x_{\text{measured}} - x_{\text{fit}}\,,$$

the intrinsic resolution of the measurement, assuming Gaussian errors can be defined as

$$\sigma_{\text{intrinsic}} = \sqrt{\sigma^2_{\text{Gaussian}} - \sigma^2_{\text{fit}}}\,,$$

where the σ_{fit} can be estimated either analytically or via a MC technique assuming the same intrinsic resolution for all ladders.

In fig. 8, the p-side residual distribution for protons is presented for a given ladder. The residual distribution is well described by the sum of two Gaussian functions, where

the $\sim 80\%$ part of data are in the narrower one. The wider Gaussian reflects the cases in which a wrong neighboring strip, due to a noise fluctuation, has been associated to the seed. The resulting η is wrong and consequently also the position measurement, worsening the resolution.

In fig. 8 is presented the position resolution function of the particle charge Z. Due to the strong dependence of η distribution to Z there are many differences between the p-side resolutions, while n-side has a constant quasi-digitalized response as expected.

8. – Conclusions

Results have been presented on the performance of the AMS-02 silicon tracker flight ladders measured in beam test conditions. Charge measurement has been achieved up to $Z = 26$. In terms of position resolution, 10 and 30 μm in the bending (p-side) and non-bending (n-side) coordinates of the AMS-02 tracker have been achieved for singly charged minimum ionizing particles. A spatial resolution of $\sim 5\,\mu$m has been measured for helium particles on the p-side. With these characteristics the tracker will be able to measure the cosmic rays rigidity until the TV region.

* * *

The work presented in this report is the result of a joint effort of the AMS-02 Tracker Collaboration. We acknowledge the contribution of all our collegues involved in the preparation of the beam test, in its successful operation and in the data analysis. In particular, we would like to thank P. Zuccon, W. J. Burger and B. Bertucci for sharing with me some of their analysis results and plots, their useful suggestions and fruitful discussions.

REFERENCES

[1] Aguilar M. *et al.*, *Phys. Rep.*, **366/6** (2002) 331.
[2] Ambrosi G. *et al.*, *Nucl. Instrum. Methods A*, **435** (1992) 215.
[3] Alpat G. *et al.*, *Nucl. Instrum. Methods A*, **540** (2005) 121.